Supplementary Material for:

Origins and Consequences of Velocity Fluctuations during DNA Passage through a Nanopore

Lu Bo[†, ‡], Fernando Albertorio[†], David P. Hoogerheide[†], and Jene A. Golovchenko[†*]

[†]Department of Physics, Harvard University, Cambridge MA 02138

[‡]Electron Microscopy Laboratory, Department of Physics, Peking University, Beijing, China

*Correspondence: golovchenko@physics.harvard.edu

The following additional appendices deal with various aspects of the modeling results presented in this paper. Appendix S1 contains all the details of the model of molecule unraveling. Appendix S2 deals with the question of dimensionality and concludes that changes in the dimensionality of the model will not be significant enough to alter the conclusions of our paper. Appendix S3 contains an extensive discussion of the magnitude of the driving force and the estimated magnitude of fluctuations in this force during translocation. Finally, Appendix S4 details how Brownian motion is added to our translocation model. All references refer to the references at the end of the supplementary material.

APPENDIX S1: DETAILS OF THE TRANSLOCATION MODEL

For the translocation process of a molecule chain, each simulation step describes the motion of one Kuhn length, or *segment*, of dsDNA through the nanopore. The index of the segment passing through the nanopore is *i*. The value of the drag coefficient γ_i depends on the details of the molecular conformation resulting from the previous step and is calculated for use in evaluating the average segment velocity $\overline{v}_i = F / \gamma_i$ and the segment translocation time $\tau_i = l_0 / \overline{v}_i$. The total translocation time for each molecule is $\tau = \sum_i \tau_i$.

The drag coefficient is calculated for the motions of the untranslocated dragged segments as they are advanced towards the nanopore. Three steps of the algorithm for updating a 14-segment molecule's geometry are depicted in Fig. S1, *A-D*. In Fig. S1*A*, we have chosen $i = 1$ for clarity. In the following discussion, a *vertex* is a joint between two segments of the molecule. The vertex number is the same as the number of the segment immediately preceding the vertex. For example, in Fig. S1*A*, the vertex to the right of segment 1 is vertex 1.

In general, the molecule will have three distinct regions of motion:

1. Part of the molecule, between the nanopore and the region of the molecule that is unraveling, is fully stretched; that is, each segment follows its preceding segment toward the nanopore without lateral motion. The vertex after the last segment corresponding to the fully stretched region we call the *unraveling point.* The unraveling points are labeled by the broken green circles in Fig. S1, *A-D*. When moving to a subsequent step, the molecular conformation between the nanopore and the current step's unraveling point remains unchanged, even though the identity of the segments in each position of this region has changed. The unraveling point changes with each step and can even move backward along the molecule.

2. Part of the molecule will be undragged. We have already introduced the *pivot point*, which separates the dragged and undragged regions of the molecule. In Fig. S1, *A-D*, the pivot points are denoted by a solid red circle. When moving to a subsequent step, the molecular conformation between the current step's pivot point and the end of the molecule remains unchanged. The pivot point, however, does change with each step but never moves backward along the molecule.
3. In the domain between the unraveling point and the pivot point, the molecule will undergo a complicated rearrangement described next.

Our simulation algorithm begins each step by identifying this third domain, which is between the unraveling and pivot points. The requirement for a domain between two vertices j and k to be rearranged during step i is that the end-to-end distance between j and k *along the molecule* (D_{jk}) must differ from the end-to-end separation of j and k *along the lattice* (L_{jk}) by either 1 or 2 Kuhn lengths. In practice, the first domain satisfying this requirement is identified by sequentially searching the vertices $k \geq i+2$ until a vertex j between i and k can be found such that $D_{jk} - L_{jk} = 1 \text{ or } 2$. The point k is then the pivot point and j is the unraveling point. Because j and k bracket the domain closest to the nanopore satisfying the rearrangement requirement, this algorithm selects the region to be updated such that the net motion of all molecule segments is minimized while allowing segment i to pass through the nanopore.

Once the unraveling and pivot points have been found, the motions of each segment can be determined. For region 1, between the nanopore and the unraveling point, each segment before the unraveling point occupies its leading segment's previous position. For region 2, after the pivot point, the segments do not move. The only complicated motion occurs between the unraveling point *j* and the pivot point *k*. The condition $D_{jk} - L_{jk} = 1$ corresponds to a geometry in which the segments between the unraveling and pivot points are not overlapped, as in Fig. S1*A*. The new molecule conformation between the unraveling point and the pivot point will describe a straight line from the unraveling point to the pivot point, as shown by comparing Fig. S1*A*, to Fig.

S1*B*. Another motion of this type occurs between Fig. S1*C*, and Fig. S1*D*. The condition $D_{jk} - L_{jk} = 2$, on the other hand, corresponds to the overlapped case in Fig. S1*B*. In this case, both segments must rotate away from their initial position, and the segment closer to the nanopore also undergoes a translation, as seen by comparing Fig. S1*B* and Fig. S1*C*. When ambiguous, as between Fig. S1*B* and Fig. S1*C*, the direction the segments rotate does not make a significant difference in the translocation time results and is chosen randomly.

The drag coefficient is calculated from the motion of each segment. It can be expressed as

$$\gamma_i = 2\pi\eta l_0 \sum_{n \geq i} C_n \,, \tag{S1}$$

where η is the solution viscosity and C_n is a dimensionless geometric factor representing the contribution of the hydrodynamic drag from the motion of the *n*th segment as the *i*th segment is pulled through the nanopore. The C_n are determined from the hydrodynamics of a rigid cylinder of diameter 2 nm and length 100 nm (one Kuhn length) at low Reynolds number (1) and can take different values depending on the motion of the segment. Possible motions with their drag contributions are: axial translation, or $n \leq j$ ($C_n = 0.27$); perpendicular translation (0.44); 60° rotation (0.22); 120° rotation (0.44); no motion (0). The effect of the nanopore walls on the segment in the nanopore is calculated from a finite element integration of the viscous force on a 2 nm cylinder in an hourglass-shaped pore of minimum radius 10 nm that approximates the geometry of our system (2); in this case $C_i = 0.52$. If C_i is chosen to be simply the drag coefficient for axial translation (0.27), the effective charge density required to fit the experimental data changes by about 10%, from 0.22 e^-/bp to 0.20 e^-/bp. For segments that experience both rotation and translation, the order of these operations is chosen to minimize the drag coefficient, though this choice has little effect on the translocation time distributions. We assume γ_i does not change and the velocity is constant during the translocation of a single segment through the nanopore. The translocation time of one molecule chain is calculated by summing the translocation times of the segments, $\tau_i = l_0 / \overline{v}_i = l_0 \gamma_i / F$.

The entire algorithm was implemented with custom MATLAB code.

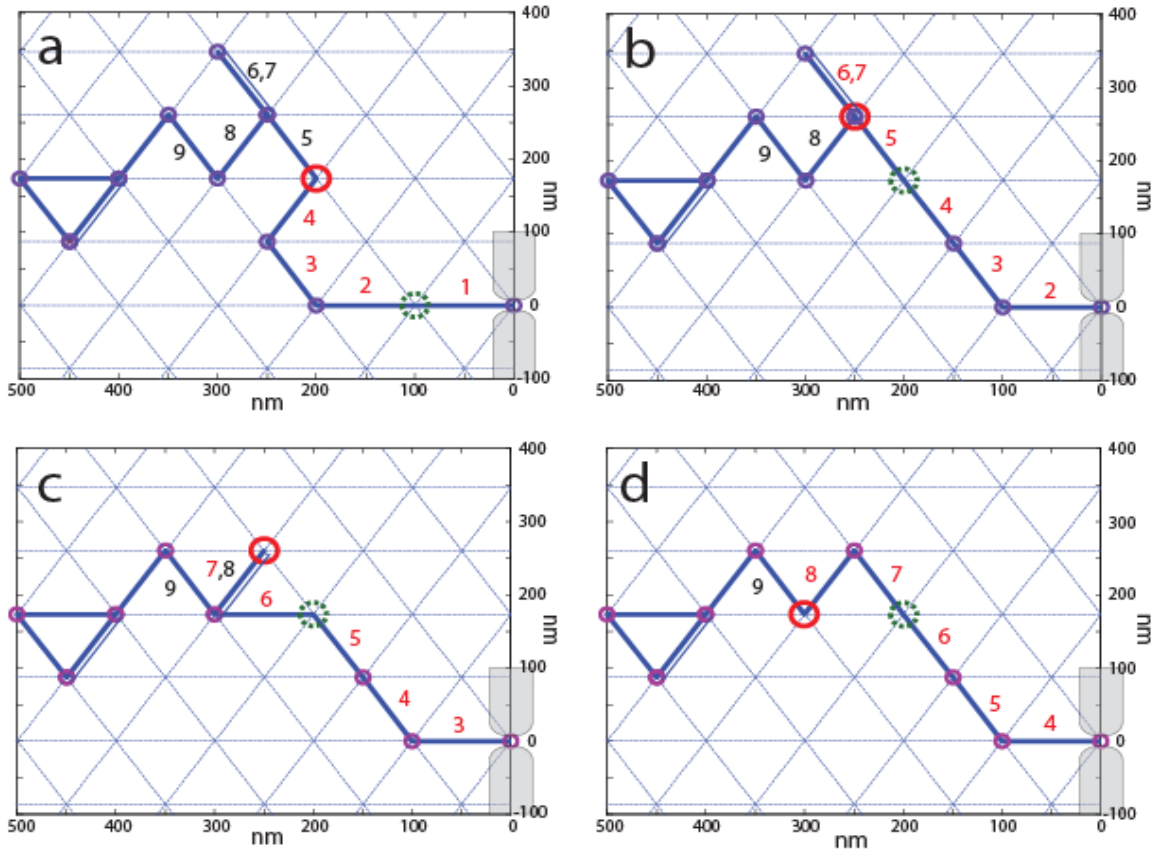

FIGURE S1. Three steps of the simulated translocation process. The DNA molecule is rendered as a freely jointed chain (blue lines; double blue lines are overlapping segments) on a two-dimensional hexagonal lattice. Each small purple circle indicates a freely rotating joint, or vertex, between two adjacent segments. Beyond the pivot point (red circle, black labels) the molecule's conformation will remain stationary on the hexagonal grid as one Kuhn length is pulled into the nanopore, while the segments with colored labels contribute to the drag force. Green, dashed circles denote the unraveling points.

APPENDIX S2. EFFECT OF DIMENSIONALITY

We expect to see some difference between a simple two-dimensional (2D) model and a full three-dimensional (3D) simulation due to the different distributions of center-of-mass distance to the nanopore (see Fig. 3 in the main text). We explored the effect of dimensionality by modifying a one-dimensional (1D) random walk model, in which the initial conformation was generated as a random walk with forward, backward, and stationary (transverse) directions. This model can be considered as quasi-2D projected to 1D if it includes one transverse dimension (with two additional directions for the random walk) and as quasi-3D if there are two transverse dimensions (each with two possible random walk directions). The translocation time distributions from the quasi-2D and quasi-3D models are compared to the results from the hexagonal 2D model in Fig. S2. As expected, because of the additional spatial degrees of freedom in the quasi-3D model, the center-of-mass distribution (and hence the translocation time) is concentrated closer to the nanopore. The differences among the three methods are not great enough to alter our conclusion that the unraveling model is sufficient to demonstrate the physics underlying the experimentally observed translocation time distributions.

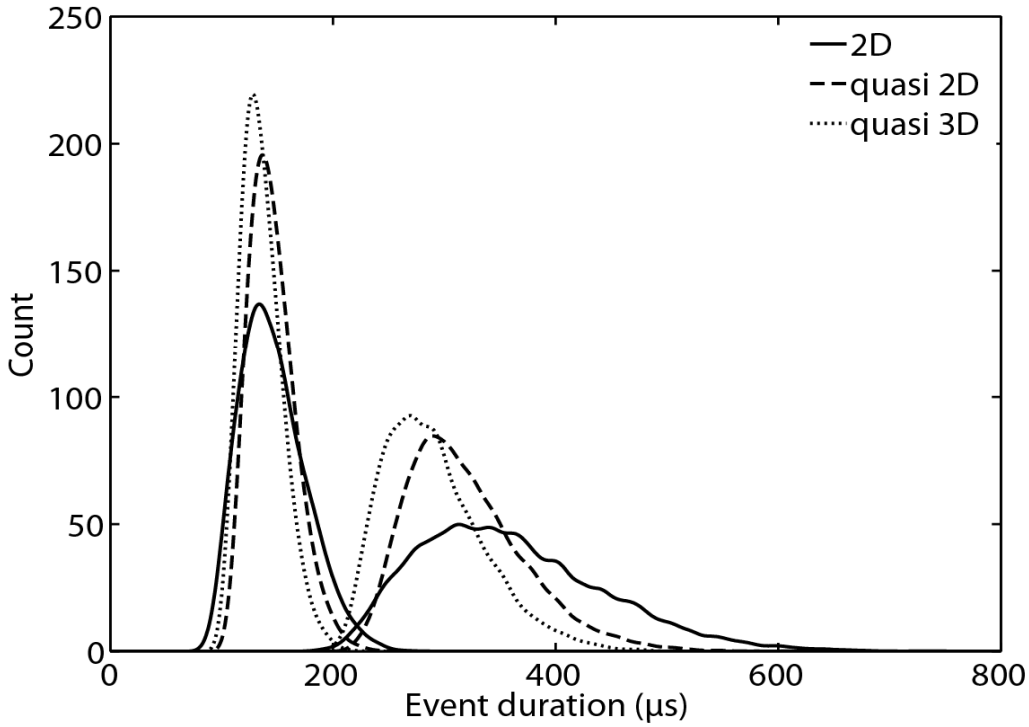

FIGURE S2. Predicted translocation time distributions from the hexagonal 2D, quasi-2D, and quasi-3D models without a center of mass offset. Curves are normalized to the same integrated area.

APPENDIX S3. THE DRIVING FORCE AND ITS FLUCTUATIONS

In the model, we assume that the driving force is constant. Here we discuss this assumption in more detail and estimate the driving force fluctuations if the molecule is not axially centered in the nanopore. In the absence of radial forces in the nanopore (a reasonable assumption more than a Debye length (0.3 nm in 1 M KCl) away from the side walls), one expects such fluctuations to occur on time scales corresponding to the radial diffusion time of a single Kuhn length in the nanopore. The relevant diffusion constant is 13×10^{-12} m^2/s (3); a typical correlation time is $R^2/D \sim 2\ \mu\mathrm{s}$, if $R \approx 5$ nm is the radius of the nanopore. This time scale is fast enough so that if the magnitude of the difference in driving force at different radial positions in the channel is large enough, the fluctuation of the driving force could in principle account for some of the observed variance in the translocation time.

The magnitude of the driving force depends primarily on the effective charge density of the DNA backbone. The bare charge of the DNA backbone is 2 electron charges per basepair (e^-/bp), and this is the charge on which the applied potential acts. The applied potential also acts on counterions that are attracted to the negative charge surface of the SiN nanopore and to the negative charge of the double strand DNA backbone. The DNA is pulled against the resulting electroosmotic flow (EOF) and moves slower than it would in the absence of the counterion flow (4). The resulting retarded motion of the DNA can be described by an effective charge density that is less than $2\ e^-/\mathrm{bp}$. Literature values for this charge density vary widely and have been measured to be anywhere from $0.10\ e^-/\mathrm{bp}$ to $0.9\ e^-/\mathrm{bp}$ (5-7). In nanopores, the EOF, and hence the effective charge, depend strongly on the surface charge state of the nanopore and therefore can be different for nanopores with different fabrication, cleaning, or wetting histories (4, 8).

The value of the charge density can be estimated from the free electrophoretic mobility measured by Nkodo et al. (9), $\mu_0 = 4.1\times10^{-8}$ m^2 / V·s . This mobility is simply the ratio of the total charge of the molecule to the total drag of the molecule, and it is found to be independent of length. If we consider a polymer as a freely jointed chain in thermal equilibrium, the total charge on the molecule is simply $Nl_0\lambda$, where N is the number of Kuhn length segments. The drag can be estimated from the fact that on average 1/3 of the molecule segments are aligned with an electric field, while 2/3 of them are transverse to the field. The total molecule drag can then be estimated from the axial and transverse drag coefficients, $\gamma_{\parallel}$ and $\gamma_{\perp}$, to be $\gamma = N\left(\gamma_{\parallel} + 2\gamma_{\perp}\right)/3$. We then obtain $\lambda = \mu_0\gamma / l_0 \approx 0.21\ e^{-}$ / bp , in good agreement with both the literature and with the charge densities found by fitting our model to the experimental result.

Different radial positions of the molecule give rise to different EOF fields in the nanopore and could in principle significantly affect the effective charge density. A simple estimate, however, shows that such fluctuations should be minimal. The EOF is generated by the electrical field acting on the region of positive charge density close to the negatively charged wall surface, so the radial gradient of the axial velocity exists only within a distance of the Debye length from the wall. With an electrolyte concentration of 1 M, the Debye length is less than 1 nm, so the enhanced drag from the EOF should be nearly constant over the width of the nanopore. We therefore expect that the effective charge density will be stable if the molecule undergoes radial position fluctuations.

APPENDIX S4: INCLUSION OF BROWNIAN MOTION IN THE COMPUTER MODEL.

The probability distribution of the one-dimensional diffusional displacement Δx of a Brownian particle with diffusion constant D after a time Δt, given an initial position $\Delta x = 0$ and uniform drift velocity $\bar{v}$, is the one-dimensional moving Gaussian kernel

$$P(\Delta x; \Delta t) = \frac{1}{\sqrt{4\pi D \Delta t}} \exp\left(-\frac{(\Delta x - \bar{v}\Delta t)^2}{4D\Delta t} \right). \quad \text{(S2)}$$

If we define the apparent diffusional velocity of the Brownian object to be $\tilde{v} = \Delta x / \Delta t$, we can write the probability distribution of the apparent velocity as

$$P(\tilde{v}; \Delta t) = \frac{\Delta t}{\sqrt{4\pi D \Delta t}} \exp\left(-\frac{(\tilde{v} - \bar{v})^2}{4D / \Delta t} \right), \quad \text{(S3)}$$

which is a Gaussian kernel centered on the uniform velocity. We use the probability distribution given in Eq. S3 to include the effects of Brownian motion in our model results. In this case, the time interval in question is the sampling interval of a hypothetical instrument, which we take to be $\Delta t = 20$ ns, the minimum sampling rate required for detecting single bases at the average molecular speeds determined by our experiments. The actual velocity of the DNA strand in the nanopore is then randomly generated from the distribution equation, Eq. S3. The velocity $\bar{v}$ and the diffusion constant $D = k_B T \bar{v} / F$ are simply those obtained from the previously described model. They vary as the molecule assumes different conformations while being pulled through the nanopore, but are assumed constant over the much smaller time scale Δt.

REFERENCES

S1. Batchelor, G. K. 1970. Slender-Body Theory for Particles of Arbitrary Cross-Section in Stokes Flow. *J. Fluid Mech.* 44:419.

S2. Kim, M. J., B. McNally, K. Murata, and A. Meller. 2007. Characteristics of solid-state nanometre pores fabricated using a transmission electron microscope. *Nanotechnology* 18:205302.

S3. Doi, M., and S. F. Edwards. 1986. The Theory of Polymer Dynamics. Oxford University Press, New York.

S4. van Dorp, S., U. F. Keyser, N. H. Dekker, C. Dekker, and S. G. Lemay. 2009. Origin of the electrophoretic force on DNA in solid-state nanopores. *Nature Physics* 5:347-351.

S5. Keyser, U. F., B. N. Koeleman, S. Van Dorp, D. Krapf, R. M. M. Smeets, S. G. Lemay, N. H. Dekker, and C. Dekker. 2006. Direct force measurements on DNA in a solid-state nanopore. *Nature Physics* 2:473-477.

S6. Schellman, J. A., and D. Stigter. 1977. Electrical Double-Layer, Zeta Potential, and Electrophoretic Charge of Double-Stranded DNA. *Biopolymers* 16:1415-1434.

S7. Smith, S. B., and A. J. Bendich. 1990. Electrophoretic Charge-Density and Persistence Length of DNA as Measured by Fluorescence Microscopy. *Biopolymers* 29:1167-1173.

S8. Ghosal, S. 2007. Electrokinetic-flow-induced viscous drag on a tethered DNA inside a nanopore. *Phys. Rev. E* 76:061916.

S9. Nkodo, A. E., J. M. Garnier, B. Tinland, H. J. Ren, C. Desruisseaux, L. C. McCormick, G. Drouin, and G. W. Slater. 2001. Diffusion coefficient of DNA molecules during free solution electrophoresis. *Electrophoresis* 22:2424-2432.